Available online at www.sciencedirect.com
ScienceDirect
Polymer 48 (2007) 5116–5124
polymer
www.elsevier.com/locate/polymer

Structure and properties of highly stereoregular isotactic poly(methyl methacrylate) and syndiotactic poly(methyl methacrylate) blends treated with supercritical CO_2

Shigeo Asai [a,*], Takatsugu Kawano [a], Shin-ichi Hirota [a], Yoichi Tominaga [a], Masao Sumita [a], Tomohiro Mizumoto [b]

[a] *Department of Chemistry and Materials Science, Tokyo Institute of Technology, 2-12-1, Ookayama, Meguro-ku, Tokyo 152-8550, Japan*
[b] *Basic Chemicals Research Laboratory, Sumitomo Chemical Co. Ltd., 5-1, Sobiraki-cho, Niihama, Ehime 792-8521, Japan*

Received 8 May 2007; received in revised form 28 June 2007; accepted 28 June 2007
Available online 10 July 2007

Abstract

The structure and properties of highly stereoregular isotactic poly(methyl methacrylate) (*it*-PMMA) and syndiotactic poly(methyl methacrylate) (*st*-PMMA) blends with crystalline stereocomplex formed by supercritical CO_2 treatment at temperatures ranging from 35 to 130 °C were investigated by means of differential scanning calorimetry (DSC), wide-angle X-ray diffraction (WAXD), and dynamic mechanical analysis (DMA) measurements. The melting temperature, T_m, and the heat of fusion, ΔH_m, had maximum values at about 200 °C and 25 J/g, respectively. The degree of crystallinity evaluated by WAXD ranged in value from 32 to 38%. The fringed-micellar stereocomplex crystallites were formed in case of treatment temperatures below 90 °C, and the orderliness perpendicular to the helix axis of the fringed-micellar crystallites was considered to be increased with increasing treatment temperature. In case of treatment temperature of 130 °C, the fringed-micellar crystallites and the lamellar crystallites with high orderliness parallel to the helix axis coupled with the perpendicular orderliness were formed, and the respective double endothermic peaks, T_m^1 and T_m^3, were observed in DSC due to the melting of the two kinds of stereocomplex crystallites. The *it*-PMMA/*st*-PMMA blends containing the fringed-micellar crystallites maintained high values of storage modulus, E', up to higher temperature compared with the amorphous blends. The E' of the blend treated with CO_2 at 130 °C decreased twice at temperatures corresponding to T_m^1 and T_m^3.

Keywords: Polymer blend; Supercritical carbon dioxide; Poly(methyl methacrylate)

1. Introduction

Stereocomplex formation between highly stereoregular isotactic poly(methyl methacrylate) (*it*-PMMA) and syndiotactic poly(methyl methacrylate) (*st*-PMMA) blends was first reported by Fox et al. in 1958 [1]. Challa and coworkers reported the blend ratio and molecular dependence on the stereocomplex formation in organic solvents or in thermal annealing [2–11]. They also reported that the stereocomplex is made of a 9/1 double-stranded helix constructed with an asymmetric unit consisting of one isotactic unit and two syndiotactic units having a pitch of 1.84 nm [11]. However, the cell parameters of the stereocomplex have not been obtained. The stereocomplex formation induced by supercritical carbon dioxide (CO_2) has been investigated by Mizumoto et al. [12–14]. They reported that the amount of the stereocomplex formed by treatment with supercritical CO_2 is found to be higher than that by thermal annealing in bulk. The crystalline stereocomplex of 33% *it*-PMMA content induced by supercritical CO_2 had only one sharp endothermic peak, while that obtained by

* Corresponding author. Tel.: +81 3 5734 2432; fax: +81 3 5734 2431.
E-mail address: asai.s.aa@m.titech.ac.jp (S. Asai).

0032-3861/$ - see front matter © 2007 Elsevier Ltd. All rights reserved.
doi:10.1016/j.polymer.2007.06.065

thermal annealing has broad melting temperatures. The sharp endothermic peak indicates a narrow distribution of sequence length and crystallite size of stereocomplex formed by supercritical CO_2. It is known that the CO_2 permeability of PMMA is relatively high compared with those of other polymers. Accordingly, the large amount of CO_2 absorbed in PMMA under the supercritical CO_2 condition increases free volume and promotes a stereocomplex formation.

The effects of CO_2 absorption into polymers have been reported by many researchers from the viewpoint of the glass transition temperature, T_g [15–17], and crystallization behavior [18–24]. For instance, Handa et al. found that the high-pressure differential scanning calorimetry (DSC) system led to a decrease of more than 40 °C in the T_g of polystyrene (PS) [17]. Several groups have reported that CO_2 is a good crystallizable agent for some polymers including PS [18], syndiotactic PS [19], poly(vinylidene fluoride) [20], poly(ethylene terephthalate) [21], polycarbonate [22], poly(phenylene sulfide) [23], and poly(ether ether ketone) [24]. Although many attempts have been made to study the crystallization behavior, there are few reports on the morphology or higher-order structure of semi-crystalline polymers crystallized with the aid of high-pressure CO_2 [25–27].

The degree of crystallinity is one of the important factors which dominate the bulk properties of semi-crystalline polymers. It is not possible to evaluate the degree of crystallinity of the crystallized sample from the heat of fusion measured by DSC, because the heat of fusion for perfect crystal of *it*-PMMA/*st*-PMMA stereocomplex has not been reported until now. On the other hand, the evaluation of the degree of crystallinity from wide-angle X-ray diffraction (WAXD) pattern requires a certain mass or a certain extent of crystalline regularity in a sample. The *it*-PMMA/*st*-PMMA stereocomplex formed by supercritical CO_2 treatment has higher crystalline regularity, which allows us to obtain a higher accuracy of the degree of crystallinity. In addition, there is little report about the higher-order structure and mechanical properties of *it*-PMMA/*st*-PMMA films with stereocomplex. In this study, the *it*-PMMA/*st*-PMMA blends at a 1/2 mixing ratio are treated with supercritical CO_2 at a wide temperature range, and we evaluate the degree of crystallinity, higher-order structure, and mechanical properties for the semi-crystallized *it*-PMMA/*st*-PMMA blends.

2. Experimental section

2.1. Materials

The *it*-PMMA sample with high stereoregularity and low molecular weight was prepared in toluene at −78 °C with *t*-BuMgBr as initiator according to a method reported by Hatada et al. [28]. The *st*-PMMA sample with high stereoregularity and high molecular weight was prepared in toluene at −78 °C with the $[Cp_2^*SmH]_2$ initiation system reported by Yasuda et al. [29]. The number-average molecular weight (M_n), the molecular weight distribution (M_w/M_n), and the tacticity of the PMMA samples prepared are listed in Table 1.

Table 1
Characteristics of the polymer samples

Sample	10^{-4} M_n[a]	M_w/M_n[a]	Tacticity (%)[b]		
			mm	mr	rr
it-PMMA	1.89	1.07	96.8	2.1	1.1
st-PMMA	48.8	1.13	0.7	9.5	89.8

[a] Measured by GPC with *at*-PMMA standards calibration.
[b] Calculated by ^{1}H NMR.

The M_n and M_w/M_n were measured by gel permeation chromatography (GPC). Tacticities (mm, mr, and rr) were determined by α-CH_3 signal intensities obtained by ^{1}H NMR spectroscopy. Details on the characterization have been reported elsewhere [12–14].

2.2. Sample preparation

The original *it*-PMMA/*st*-PMMA blend films were prepared by casting a 5 wt% dichloromethane solution of *it*-PMMA and *st*-PMMA in the mixing weight ratio of *it*-PMMA/*st*-PMMA = 1/2 in a petri dish. To remove all solvent, the film was dried for 1 day at room temperature and afterward dried for 1 day at 40 °C under vacuum. Before treatment with supercritical CO_2 or thermal treatment, all films were heated at 250 °C for 5 min and pressed under a pressure of 29.4 MPa for 2 min and then quenched into ice water to obtain quenched films without any solvent or thermal histories. The film thickness was 0.5 mm. The *it*-PMMA films and *st*-PMMA films were also prepared using the same method as described above.

2.3. Supercritical CO_2 treatment and thermal treatment procedure

Supercritical CO_2 treatment was conducted using a supercritical CO_2 extraction system (JASCO Corp., Japan) consisting of a delivery pump (SCF-Get), an automatic backpressure regulator (SCF-Bpg) and a heater. The sample of quenched films were introduced into an autoclave (50 ml) made of stainless steel (SUS) and kept at a constant temperature. Liquid CO_2 was pumped into the autoclave from the delivery pump at a rate of 10 ml/min, and the autoclave was maintained at a constant pressure with a CO_2 flow rate of 2 ml/min. The treatment temperature was varied between 35 and 130 °C, and the treatment pressure was 20 MPa. After treatment for 8 h, the autoclave was slowly cooled to room temperature to avoid the films from being foamed, and depressurized. After taking out the films from the autoclave, they were dried in vacuum at 30 °C for at least 3 days to remove CO_2.

The re-annealed sample was prepared from the supercritical CO_2 treatment film by thermal treatment under ambient pressure in air at a temperature of 170 °C using a FP80HT hot stage (Mettler Toledo) for 15 min followed by quenching into ice water. In addition, annealed samples were prepared from as-quenched amorphous films by thermal treatment in air at a temperature of 150 °C using an FP80HT for 15 days followed by quenching into ice water.

The drawn films were prepared from the as-quenched films drawn at a temperature of 100 °C using a uni-axial drawing machine (homemade) in a draw ratio of 3 followed by drying in vacuum at 30 °C for 1 day. The supercritical CO_2 treatment of the drawn films was carried out using the same procedure as described above with both ends of the film fixed. The CO_2 treatment conditions of temperature, pressure, and time are 130 °C, 20 MPa, and 8 h, respectively.

2.4. Measurements

Differential scanning calorimetry (DSC) measurements were carried out using a DSC-50 (Shimadzu Corp., Japan) in the temperature range from −10 to 250 °C at a heating rate of 20 °C/min under nitrogen gas atmosphere. The melting temperature, T_m, was determined from the maximum of the melting endothermic peak. The heat of fusion, ΔH_m, was determined by the peak area of the melting endotherm. At a heating rate of 5 °C/min, DSC measurements were also performed to compare with the temperature dispersion of storage modulus evaluated from the dynamic mechanical analysis measured at the same heating rate, 5 °C/min as described below.

Wide-angle X-ray diffraction (WAXD) measurements were carried out using a RINT-2100 system (Rigaku Corp., Japan) with Cu Kα radiation ($\lambda = 0.15418$ nm) operating at 40 kV and 40 mA. The system was equipped with a pin-hole collimator and a graphite monochromator in a scattering beam line, and the X-ray intensity was measured in a symmetrical-transmission (θ–2θ) mode within the range of 2θ from 2° to 60° using a scintillation counter. The measured intensity was corrected for air scattering, absorption factor, and polarization factor.

Two-dimensional WAXD pattern was measured using a RU-200 and R-AXIS-DS3 imaging plate (IP) system (Rigaku Corp., Japan). The Cu Kα radiation ($\lambda = 0.15418$ nm) with operating power of 50 kV and 180 mA was used and the monochromatic X-ray beam was obtained by an incident type monochromator CN1707 (Rigaku Corp., Japan) and collimated by a pin-hole collimator. An IP film (Fujifilm BAS-SR 127) was used as a two-dimensional flat-film detector and the resolution (pixel size) was set to 50 μm in *R*-AXIS-DS3. The camera length, that is the distance between sample and an IP film, was determined by the reflections of silicon powder as a standard. First, a constant value as background, which is an offset for zero-level intensity, was subtracted from measured intensity, and next, the intensity at each pixel was corrected for a distance between sample and each pixel on a flat IP film. In the case of isotropic sample, to obtain an intensity curve against scattering angle (2θ), the intensity was averaged throughout the whole azimuth angle at the same 2θ position on the IP film. Finally, the intensity corrections for air scattering, absorption factor, polarization factor, and incoherent scattering were performed.

Dynamic mechanical analysis (DMA) was carried out with a DVA-200S (ITK Co., Japan). The size of test pieces was 5 mm in width, 30 mm in length, and 0.5 mm in thickness. This measurement was performed in a tension mode with 0.05% strain amplitude at a frequency of 10 Hz. The temperature ranged from 25 to 250 °C with a heating rate of 5 °C/min.

3. Results and discussion

3.1. Miscibility

To confirm the miscibility between *it*-PMMA and *st*-PMMA, DSC measurements were performed. Fig. 1 shows the DSC thermogram of the quenched film of *it*-PMMA/*st*-PMMA (1/2 wt/wt) blend. The data for *it*-PMMA and *st*-PMMA films are also shown for reference. The arrows in this figure indicate the midpoint of grass transition temperature, T_g. The absence of the endothermic peaks corresponding to the melting of crystals is an evidence for the amorphous nature of those quenched films. The amorphous nature of the films was also revealed by the WAXD profile as described below. The amorphous *it*-PMMA/*st*-PMMA 1/2 blend, in particular, showed a single T_g between those of *it*-PMMA and *st*-PMMA. This indicates that the *it*-PMMA/*st*-PMMA 1/2 blend is miscible in an amorphous state.

3.2. CO_2-induced crystallization behavior

To investigate the effect of the treatment temperature on crystallization behavior, amorphous *it*-PMMA/*st*-PMMA blend films were treated with supercritical CO_2 for 8 h at various temperatures under a constant pressure of 20 MPa. Fig. 2 shows the WAXD profiles of the *it*-PMMA/*st*-PMMA blend films crystallized by supercritical CO_2 treatment at temperatures in the 35–130 °C range. The WAXD profile of amorphous film, which is also shown for reference, possesses an

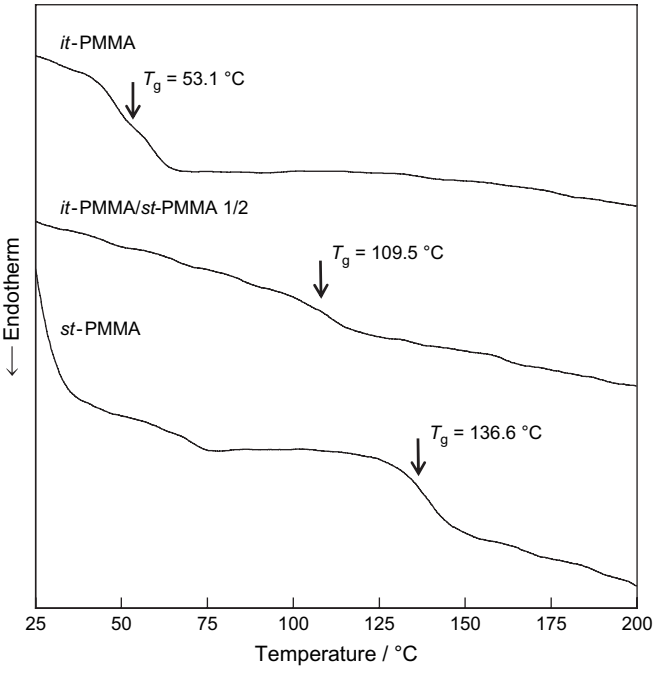

Fig. 1. DSC thermograms of as-quenched (amorphous) films of *it*-PMMA, *st*-PMMA, and *it*-PMMA/*st*-PMMA (1/2 wt/wt) blend. Heating rate, 20 °C/min.

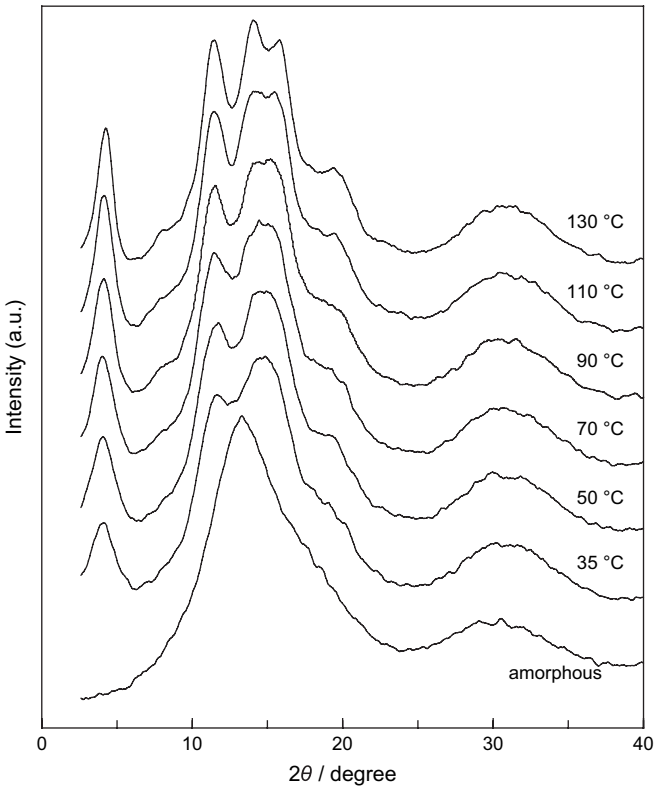

Fig. 2. WAXD profiles of *it*-PMMA/*st*-PMMA (1/2 wt/wt) blend films treated with supercritical CO_2 at temperatures in the 35–130 °C range. The bottom line is WAXD profile of as-quenched (amorphous) *it*-PMMA/*st*-PMMA blend film.

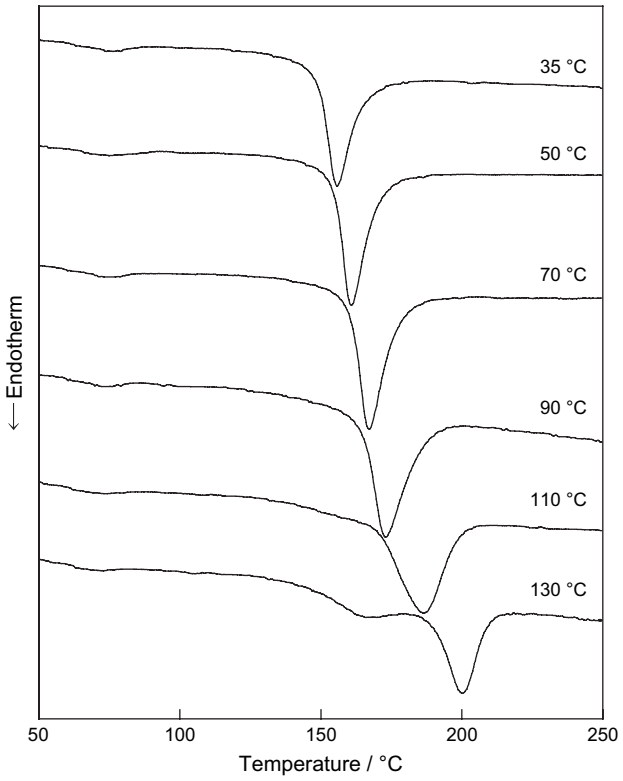

Fig. 3. DSC thermograms of *it*-PMMA/*st*-PMMA (1/2 wt/wt) blend films treated with supercritical CO_2 at temperatures in the 35–130 °C range.

amorphous halo without any crystalline diffraction peaks. The diffraction peaks were observed at 4.3°, 11.5°, 14.1°, 15.8°, and 19.4° in the profiles for the blend films treated with supercritical CO_2, and these peaks increased in intensity and narrowed with the increase of treatment temperatures. These diffraction peaks were assigned to *it*-PMMA/*st*-PMMA stereocomplex [7]. The diffraction peak at 8.6°, corresponding to *it*-PMMA crystalline structure [30,31], was not observed on the WAXD profiles of the *it*-PMMA/*st*-PMMA blend films treated with supercritical CO_2. The obtained profiles showed the evidence of the crystalline stereocomplex of *it*-PMMA/*st*-PMMA induced by supercritical CO_2 treatment.

Fig. 3 shows the DSC thermograms of the *it*-PMMA/*st*-PMMA (1/2 wt/wt) blend films crystallized by supercritical CO_2 treatment at temperatures, between 35 and 130 °C. The endothermic peaks ($\Delta H_m \sim 20$ J/g), which were attributed to the heat of fusion of the stereocomplex induced by supercritical CO_2 [12], were observed at about 150–200 °C. Fig. 4 gives T_m and ΔH_m of the stereocomplex as a function of treatment temperature. The T_m increased with the increase in the treatment temperature, especially at temperatures higher than 90 °C. It is reported that the T_m of the stereocomplex increases as the dimensions (sequence length) develop and quality of the crystalline complexes is improved [10]. Therefore, in case the treatment temperature is above 90 °C, it is considered that the stereocomplex with long sequence length and higher quality is formed. This coincides with the WAXD result that the diffraction peak at 4.3° becomes larger and sharper with the increase in the treatment temperature. When the treatment temperature was 130 °C, double endothermic peaks were observed at around 165 and 200 °C, and it is discussed later.

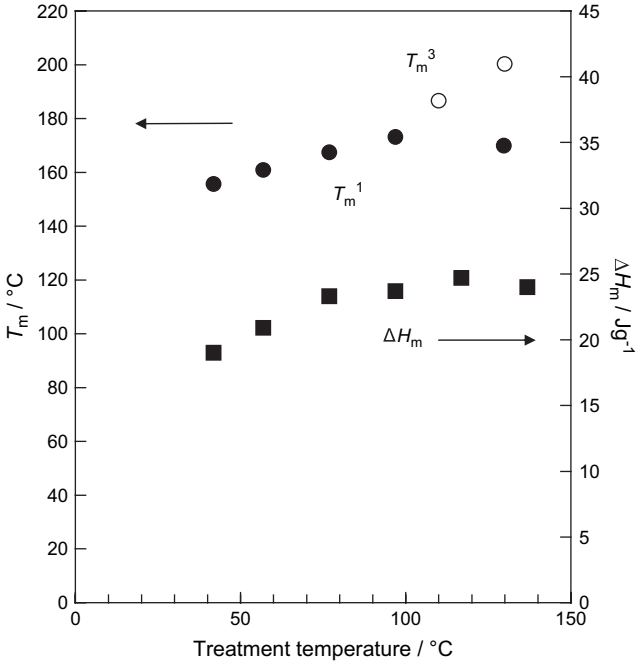

Fig. 4. T_m (T_m^1 (●), T_m^3 (○)) and ΔH_m (■) as a function of CO_2 treatment temperature.

3.3. The degree of crystallinity

The degree of crystallinity is one of the important and necessary factors to discuss the bulk properties of semi-crystalline polymers. The *it*-PMMA/*st*-PMMA stereocomplex crystallites with higher regularity are formed by supercritical CO_2 treatment and give rise to the clear WAXD profiles as shown in Fig. 2, which allow us to obtain a higher accuracy value of the degree of crystallinity from WAXD data. Fig. 5 shows the degree of crystallinity, which is evaluated by separating crystalline reflections from total WAXD curve, as a function of CO_2 treatment temperature. The degree of crystallinity increased with rising treatment temperature up to 90 °C and almost became leveling off in temperatures higher than 90 °C. This tendency corresponded to the treatment temperature dependence of ΔH_m by DSC as shown in Fig. 4.

3.4. Dynamic mechanical analysis

To discuss the mechanical properties of *it*-PMMA/*st*-PMMA (1/2 wt/wt) blend, the temperature dispersion of storage modulus (E') was obtained by a DMA measurement. Fig. 6 shows a temperature dispersion of E' and a DSC thermogram measured with a heating rate of 5 °C/min for the amorphous *it*-PMMA/*st*-PMMA blend. The decrease of E' was observed at temperatures from 60 to 140 °C due to the α-relaxation. On the other hand in Fig. 7, the E' did not change at around T_g, but it decreased twice at higher temperatures corresponding to the melting of stereocomplex crystallites in case of the *it*-PMMA/*st*-PMMA blend crystallized by supercritical CO_2 treatment at 130 °C. It must be noted that the slight difference between the T_m^1 and T_m^3 in Fig. 7 (5 °C/min) and that in Fig. 3 (20 °C/min) for the sample treated at 130 °C is due to the difference in the heating rate of DSC measurements. To demonstrate the influence of treatment temperature on the mechanical properties, the DMA data for several samples were compared. Fig. 8 shows the temperature dispersion of E' for the amorphous *it*-PMMA/*st*-PMMA blend and the blend treated with supercritical CO_2 at 35, 90, and 130 °C. The *it*-PMMA/*st*-PMMA blend with crystalline stereocomplex inhibited the decrease in E' at around T_g due to the α-relaxation, and maintained its high value of E' up to the melting temperature of stereocomplex. The *it*-PMMA/*st*-PMMA blends treated with supercritical CO_2 had degree of crystallinity less than 40%, indicating that they have an amorphous fraction of more than 60%. The fact that the blend films maintained their high value of E' up to higher temperature in spite of the large amount of an amorphous phase is considered to suggest that there is small fringed-micellar clusters of

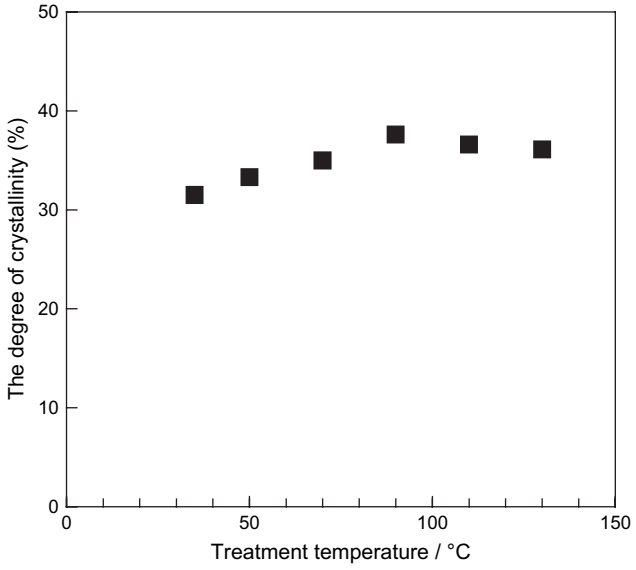

Fig. 5. The degree of crystallinity as a function of CO_2 treatment temperature.

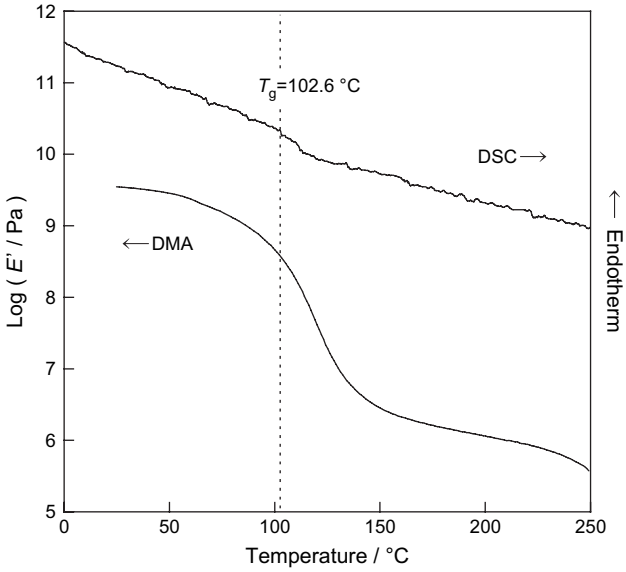

Fig. 6. Temperature dispersion of E' and DSC thermogram of amorphous *it*-PMMA/*st*-PMMA blend film. Heating rate, 5 °C/min.

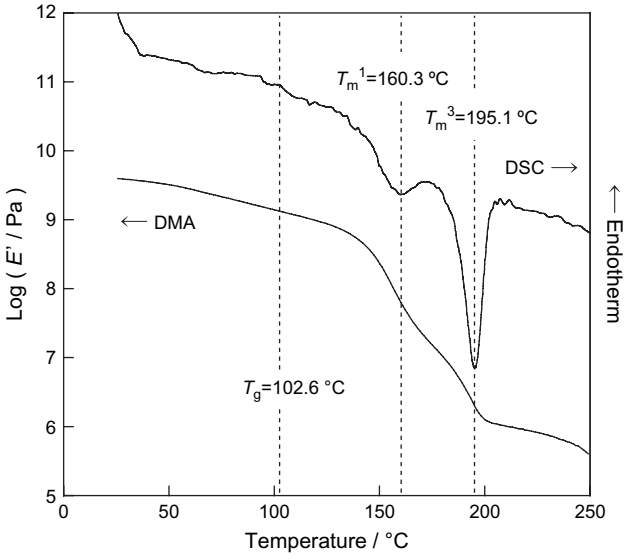

Fig. 7. Temperature dispersion of E' and DSC thermogram of *it*-PMMA/*st*-PMMA (1/2 wt/wt) blend film treated with supercritical CO_2 at 130 °C. Heating rate, 5 °C/min.

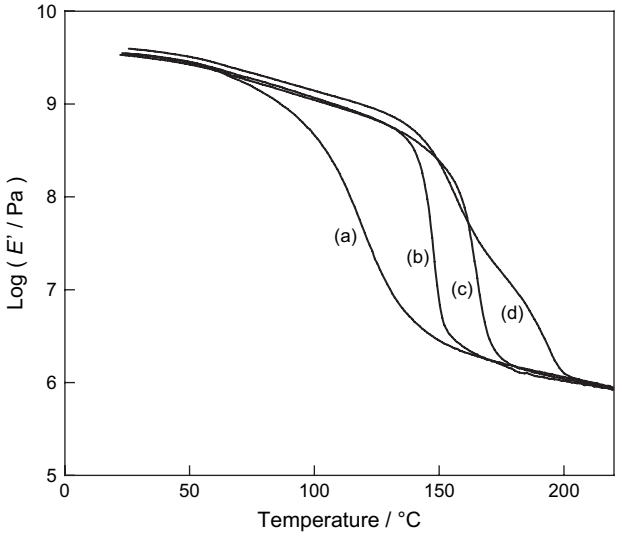

Fig. 8. Temperature dispersion of E' for (a) amorphous *it*-PMMA/*st*-PMMA blend (1/2 wt/wt) film and the blend films treated with supercritical CO_2 at (b) 35 °C, (c) 90 °C, and (d) 130 °C. Heating rate, 5 °C/min.

stereocomplex, which do not contribute to the crystalline reflections in WAXD, in the amorphous phase. Another possible explanation for the high value in E' at higher temperatures than T_g is that the restriction of molecular motion in amorphous phase, especially in the amorphous near the interface with the stereocomplex crystallites, inhibits the large decrease in E′.

3.5. Thermal annealing after supercritical CO_2 treatment

For the investigation of the melting behavior and structure of the *it*-PMMA/*st*-PMMA blend film treated with CO_2 at 130 °C (130 °C CO_2-treated sample), which has two endothermic peaks due to melting of stereocomplex crystallites at around 165 and 200 °C in the DSC thermogram as shown in Fig. 3, we prepared the following two samples. The re-annealed sample was prepared by annealing the 130 °C CO_2-treated sample at 170 °C, and the annealed sample was prepared by annealing the original amorphous film at 150 °C in air as described in the experimental section. Fig. 9 shows the DSC thermograms of the 130 °C CO_2-treated sample, the re-annealed sample, and the annealed sample. In contrast to the 130 °C CO_2-treated sample which possesses double endothermic peaks, the re-annealed sample has only one endothermic peak at 200 °C, indicating that the stereocomplex crystallites with lower melting point in the CO_2-treated sample melted by annealing at 170 °C. The endothermic peak at around 200 °C of the re-annealed sample is sharper than that of the annealed sample, suggesting that the distribution of sequence length in stereocomplex of re-annealed sample is narrower than that of annealed sample. This means that the supercritical CO_2 treatment can form the stereocomplex crystallites with higher stability in a shorter period of time compared with the thermal annealing treatment under ambient pressure in air. Next, WAXD measurements were conducted

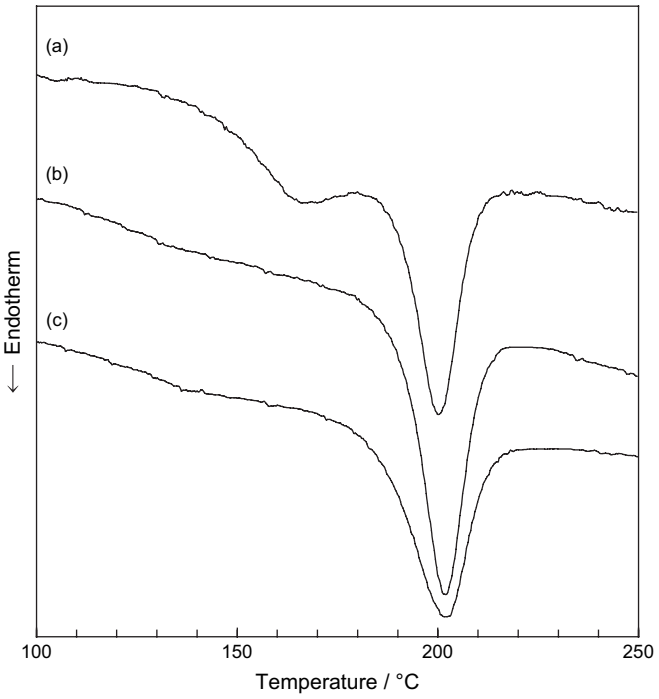

Fig. 9. DSC thermograms of *it*-PMMA/*st*-PMMA (1/2 wt/wt) blend films. (a) CO_2-treated (130 °C) sample, (b) re-annealed (170 °C) sample, (c) annealed (150 °C) sample.

to investigate the difference in structure of the three samples, and the WAXD profiles are shown in Fig. 10. The thermal annealing at 170 °C in air accompanying the CO_2 treatment at 130 °C induced a diminution of three peaks at 4.3°, 11.5°,

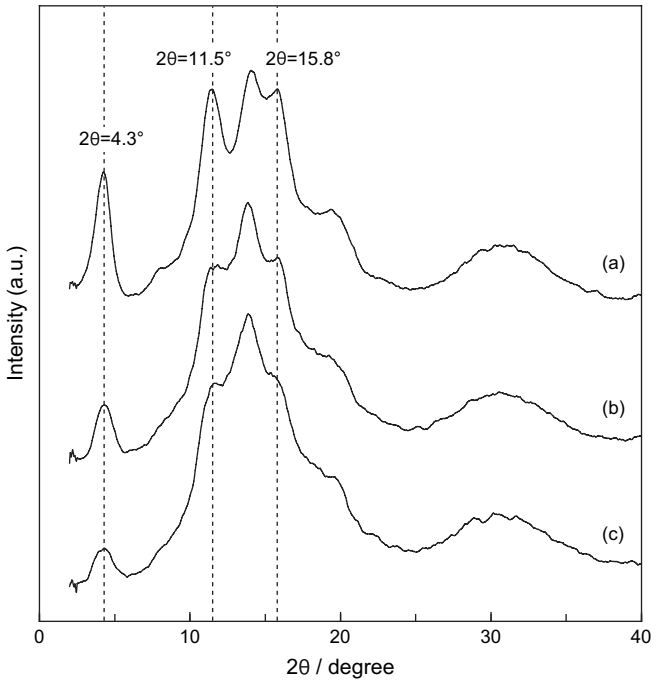

Fig. 10. WAXD profiles of *it*-PMMA/*st*-PMMA (1/2 wt/wt) blend films. (a) CO_2-treated (130 °C) sample, (b) re-annealed (170 °C) sample, (c) annealed (150 °C) sample.

and 15.8° in the WAXD. That is, by annealing the CO_2-treated sample at 170 °C, the melting endotherm at lower temperature disappeared in DSC and the intensity of the three reflections decreased in WAXD. It is necessary to assign those crystalline reflections in order to elucidate the fine structure of the 130 °C CO_2-treated sample which has double endothermic peaks in DSC. For the assignment, we prepared the *it*-PMMA/*st*-PMMA blend film with molecular oriented crystalline stereocomplex by using a drawn film as described in the experimental section, and measured two-dimensional WAXD pattern as shown in Fig. 11. The diffraction angle (2θ) and the Bragg's spacing (d) for observed reflections are listed in Table 2. The WAXD fiber pattern and the reflection data are in agreement with previous data by Challa and coworkers [7]. Three peeks are observed at 4.5°, 11.7°, and 15.8° on the equator, if fiber axis of crystallites coincides with the draw direction; they are assigned to the reflections from the planes parallel to the helix (molecular) axis. The peak positions of these peaks are in agreement with those of the three peaks which were decreased by the thermal annealing at 170 °C as shown in Fig. 10. Therefore, the three decreased peaks are assigned to the reflections from the planes parallel to the helix axis. These results indicate that the orderliness perpendicular to the helix axis decreases by the thermal annealing at 170 °C, that is, the stereocomplex crystallites with the lower melting temperature (T_m^1) have the orderliness perpendicular to the helix axis, but they melt by annealing at 170 °C, probably due to the less orderliness parallel to the helix axis. On the other hand, the stereocomplex crystallites, which have the orderliness parallel to the helix axis and the higher melting temperature (T_m^3), survive after annealing at 170 °C and possess the strong reflection at 14.1°, which corresponds to the reflection of second layer line at 13.9° in Fig. 11, as shown in Fig. 10(b) of re-annealed sample.

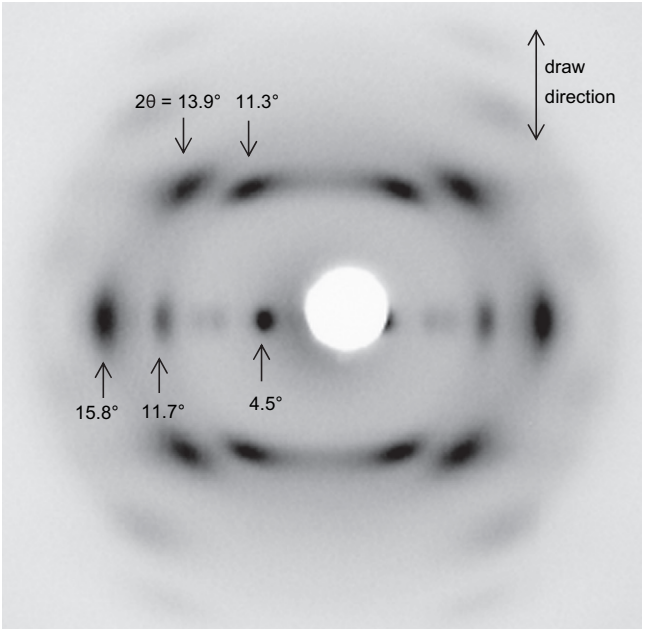

Fig. 11. Two-dimensional WAXD pattern of molecular oriented crystalline stereocomplex of *it*-PMMA/*st*-PMMA (1/2 wt/wt) blend.

Table 2
Observed reflections in the WAXD fiber pattern of the drawn film of *it*-PMMA/*st*-PMMA (1/2) blend treated with supercritical CO_2

Layer line	2θ/degree	d/nm	Intensity
$l=0$	4.5	1.96	Strong
	11.7	0.76	Strong
	15.8	0.56	Strong
$l=2$	11.3	0.78	Strong
	13.9	0.64	Strong

3.6. Structure of it-PMMA/st-PMMA blend with stereocomplex

According to the mechanistic model proposed by Schomaker et al. [9], the stereocomplex crystallites with lower (T_m^1) and higher (T_m^3) melting temperatures correspond to the fringed-micellar structure and the lamellar crystallites, respectively. We have to point out the discrepancy between the Schomaker's results and our results, especially in WAXD data. In their report, the fringed-micellar crystallites with T_m^1 are only small bundles of helices, in which the orderliness parallel to the helix axis dominates the diffraction pattern without the strong ''equatorial'' reflections. In addition, the lamellar crystallites with T_m^3 have the orderliness perpendicular to the helix axis resulting in strong ''equatorial'' reflections. In case of our results, the fringed-micellar crystallites with T_m^1 contribute to the ''equatorial'' reflections, indicating the same or higher degree of orderliness perpendicular to the helix axis, compared with lamellar crystallites. The lamellar crystallites with T_m^3 have the orderliness parallel to the helix axis coupled with the perpendicular orderliness, leading them to have the higher melting temperature. Such discrepancies, i.e. the difference of orderliness in the fringed-micellar crystallites, may arise from the difference in the preparation methods for samples with stereocomplex, i.e., the supercritical CO_2 treatment used in our method. Therefore, in order to explain our results according to the Schomaker's mechanistic model, we need some broad interpretation of the model as follows. In case of the samples with stereocomplex made by the supercritical CO_2 treatment in this study, the fringed-micellar crystallites are formed in case of treatment temperatures below 90 °C, and two kinds of crystallites, i.e., the fringed-micellar crystallites and lamellar crystallites, are formed when the treatment temperatures are 130 °C and probably 110 °C. In case the treatment temperature is 130 °C, the fringed-micellar crystallites seem to be formed during the secondary crystallization, because only fringed-micellar growth is possible after the decreasing mobility of amorphous molecules due to the primary growth of lamellar structure [9]. Regarding the effect of CO_2 treatment temperature on the structure of stereocomplex crystallites, the orderliness perpendicular to the helix axis of the fringed-micellar crystallites with T_m^1 is considered to be increased with the increase in the treatment temperature. As a result, the intensity of ''equatorial'' reflections of 4.3°, 11.5°, and 15.8° increase and the T_m^1 rises gradually with treatment temperature as shown in Figs. 2 and 3, respectively. Especially in case of treatment temperature of 130 °C, the

existence of the fringed-micellar crystallites with high orderliness perpendicular to the helix axis, which contribute to the strong ''equatorial'' reflections, is confirmed by the re-annealing experiment as stated above, the data of which are shown in Fig. 10. In addition, the larger increase in the melting temperature is observed at treatment temperatures above 110 °C as shown in Fig. 4, and the increase of reflection at 14.1° is recognized at treatment temperature of 130 °C, indicating the formation of the lamellar crystallites with high orderliness parallel to the helix axis coupled with the perpendicular orderliness.

Finally, we discuss the relation between the semi-crystalline structure and the mechanical properties. Fig. 12 shows the temperature dispersion of E' for the same *it*-PMMA/*st*-PMMA blend films as those in Figs. 9 and 10. The data of amorphous sample is also shown in Fig. 12(d). The E' of the blend film treated with CO_2 at 130 °C (a) decreases twice at temperatures corresponding to the melting of fringed-micellar and lamellar crystallites of stereocomplex as stated above. The 130 °C CO_2-treated sample maintains high values of E' up to higher temperature compared with other three samples. This is mainly due to the existence of fringed-micellar crystallites, which hinder the mobility of the noncomplexed chain sections in amorphous phase. Such a hindrance on molecular mobility by the fringed-micellar crystallites is also discussed in literature from the viewpoint of the influence on the glass transition temperature [9]. Furthermore, re-annealed sample and annealed sample still maintain high values of E' up to higher temperature compared with amorphous sample. This may be due to the existence of small fringed-micellar clusters, which are not crystallites, of stereocomplex in the amorphous phase and/or the restriction of molecular motion in amorphous phase by the presence of the stereocomplex lamellar crystallites as discussed in Fig. 8. Another point which should be mentioned is that there is good agreement between the temperature dispersion of E' for re-annealed sample (b) and that for annealed sample (c). This result is consistent with the result that the two samples have similar DSC curves and WAXD patterns as shown in Figs. 9 and 10, respectively.

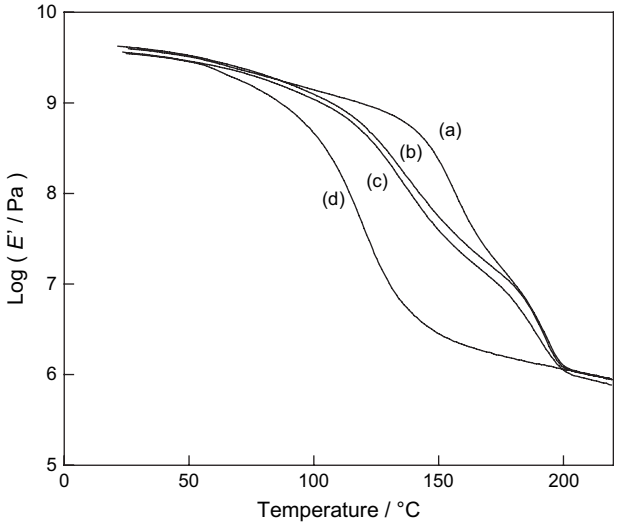

Fig. 12. Temperature dispersion of E' for *it*-PMMA/*st*-PMMA (1/2 wt/wt) blend films. (a) CO_2-treated (130 °C) sample, (b) re-annealed (170 °C) sample, (c) annealed (150 °C) sample, (d) amorphous sample.

4. Conclusions

The structure and properties of highly stereoregular *it*-PMMA and *st*-PMMA blends with crystalline stereocomplex formed by supercritical CO_2 treatment at wide temperature range, from 35 to 130 °C, were investigated by means of DSC, WAXD, and DMA measurements. The *it*-PMMA/*st*-PMMA blend with weight ratio of 1/2 was a miscible blend showing single T_g between those of *it*-PMMA and *st*-PMMA. With the increase in the treatment temperature, the intensity of the reflections assigned to stereocomplex crystallites increased, and the melting temperature, T_m, and heat of fusion, ΔH_m, also showed an increase. In the experimental condition, T_m and ΔH_m had maximum values at about 200 °C and 25 J/g, respectively. The degree of crystallinity was evaluated from WAXD data, and it ranged in value from 32 to 38%. The structure of crystalline stereocomplex in the *it*-PMMA/*st*-PMMA blends treated with supercritical CO_2 was discussed based on the data of re-annealing experiment and the mechanistic model proposed by Schomaker and Challa [9] as a function of treatment temperature. The fringed-micellar crystallites were formed in case of treatment temperatures below 90 °C, and the orderliness perpendicular to the helix axis of the fringed-micellar crystallites was considered to be increased with increasing treatment temperature. As a result, the intensity of ''equatorial'' reflections of 4.3°, 11.5°, and 15.8° in WAXD increased and the melting temperature for the fringed-micellar crystallites, T_m^1, rose gradually with increasing treatment temperature. In case of treatment temperature of 130 °C, two kinds of crystallites, i.e., the fringed-micellar crystallites and lamellar crystallites were formed, and double endothermic peaks, T_m^1 and T_m^3, were observed in DSC due to the melting of the two kinds of stereocomplex crystallites. The existence of the lamellar crystallites with high orderliness parallel to the helix axis coupled with the perpendicular orderliness resulted in the larger increase in the melting temperature and the increase of reflection at 14.1°. The *it*-PMMA/*st*-PMMA blends with the fringed-micellar stereocomplex crystallites maintained high values of storage modulus, E', up to higher temperature compared with amorphous samples, due to the restriction effect on the mobility of the noncomplexed chain sections in amorphous phase by the fringed-micellar crystallites. The E' of the blend film treated with CO_2 at 130 °C decreased twice at temperatures corresponding to T_m^1 and T_m^3.

References

[1] Fox TG, Garrett BS, Goode WE, Gratch S, Kincaid JF, Spell A, et al. J Am Chem Soc 1958;80:1768–9.
[2] Buter R, Tan YY, Challa G. J Polym Sci Polym Chem Ed 1973;11:2975–89.
[3] Feitsma EL, de Boer A, Challa G. Polymer 1975;16:515–9.
[4] de Boer A, Challa G. Polymer 1976;17:633–7.

[5] Vorenkamp EJ, Bosscher F, Challa G. Polymer 1979;20:59–64.
[6] Vorenkamp EJ, Challa G. Polymer 1981;22:1705–8.
[7] Bosscher F, Brinke GT, Challa G. Macromolecules 1982;15:1442–4.
[8] Schomaker E, Vorenkamp EJ, Challa G. Polymer 1986;27:256–60.
[9] Schomaker E, Challa G. Macromolecules 1988;21:2195–203.
[10] Schomaker E, Hoppen H, Challa G. Macromolecules 1988;21:2203–9.
[11] Schomaker E, Challa G. Macromolecules 1989;22:3337–41.
[12] Mizumoto T, Sugimura N, Moritani M, Sato Y, Masuoka H. Macromolecules 2000;33:6757–63.
[13] Mizumoto T, Sugimura N, Moritani M, Sato Y, Masuoka H. Macromolecules 2001;34:1291–6.
[14] Mizumoto T, Sugimura N, Moritani M, Yasuda H, Sato Y, Masuoka H. Macromolecules 2001;34:5200–4.
[15] Condo PD, Sanchez IC, Panayiotou CG, Johnston KP. Macromolecules 1992;25:6119–27.
[16] Condo PD, Johnston KP. Macromolecules 1992;25:6730–2.
[17] Handa YP, Capowski S, O'Neill M. Thermochim Acta 1993;226:177–85.
[18] Shieh YT, Su JH, Manivannan G, Lee PHC, Sawan SP, Spall WD. J Appl Polym Sci 1996;59:695–705.
[19] Handa YP, Zhang Z. Macromolecules 1997;30:8505–7.
[20] Chiou JS, Barlow JW, Paul DR. J Appl Polym Sci 1985;30:3911–24.
[21] Mizoguchi K, Hirose T, Naito Y, Kamiya Y. Polymer 1987;28:1298–302.
[22] Fleming GK, Koros WJ. Macromolecules 1986;19:2285–91.
[23] Schultze TD, Engelmann IAD, Boehning M, Springer J. Polym Adv Tech 1991;2:123–6.
[24] Handa YP, Roovers J, Wang F. Macromolecules 1994;27:5511–6.
[25] Asai S, Shimada Y, Tominaga Y, Sumita M. Macromolecules 2005;38:6544–50.
[26] Hirota S, Sato T, Tominaga Y, Asai S, Sumita M. Polymer 2006;47:3954–60.
[27] Koga Y, Saito H. Polymer 2006;47:7564–71.
[28] Hatada K, Ute K, Tanaka K, Kitayama T, Okamoto Y. Polym J 1985;17:977–80.
[29] Yasuda H, Yamamoto H, Yokota K, Miyake S, Nakamura A. J Am Chem Soc 1992;114:4908–10.
[30] Könnecke K, Rehage G. Colloid Polym Sci 1981;259:1062–9.
[31] Bosscher F, Brinke GT, Eshuis A, Challa G. Macromolecules 1982;15:1364–8.